

# Fluorescent Cadmium Chalcogenide Nanoclusters in Ubiquitin

Özlem Akyüz, Martin Scheffner, and Helmut Cölfen\*

Fluorescent semiconductor nanoclusters (FNCs) have received much attention by many scientists due to their attractive functions and features. However, the traditional organometallic chemical synthesis routes for such FNCs require harsh reaction conditions in organic solvents, which limit their use in biological applications. Therefore, developing synthesis strategies for the fabrication of FNCs by association with proteins under mild reaction conditions is pivotal to improve their functionalities. In addition, understanding the effect of structural and chemical properties of proteins on the synthesis mechanism of FNCs is one of the key points, which eventually enables to control and tune the photophysical properties of FNCs. The purpose of this study is to introduce the syntheses of cadmium selenide nanocluster (CdSeNC) and cadmium sulfide nanocluster (CdSNC) by using ubiquitin, a small cysteine-free protein, and investigating their properties via spectroscopic and microscopic methods. It is shown that significant changes in the protein structure as well as in its oligomerization occur upon the formation of the highly hydrated FNCs.

## 1. Introduction

The fabrication of functional, advanced, and even “smart” organic/inorganic hybrid nanomaterials (NMs) with potential applications in chemical and biological sensing,<sup>[1]</sup> theranostics,<sup>[2]</sup> imaging,<sup>[3]</sup> and catalysis<sup>[4]</sup> has received much attention in the past few decades. A number of various syntheses routes have emerged to obtain the most efficient chemical and physical

properties of such NMs. In this article, bio-inspired synthesis methods have garnered our attention due to their low-cost, nontoxicity, and eco-friendly reaction conditions allowing the use of ambient temperature and pressure in aqueous environments.<sup>[5]</sup> In addition, size, shape, and morphology of the NMs can be controlled by tuning the properties of the biomolecules used in the synthesis. A broad range of biomolecules can be utilized for the synthesis of NMs such as proteins<sup>[6]</sup> and peptides<sup>[7]</sup> that have a crucial role in direction-controlled formation of nanostructures depending on their 3D structures and sequence-specific binding properties. The most prominent example of protein-controlled formation of inorganic structures is the process of biomineralization with multiple control handles of proteins and their superstructures for the controlled nucleation, growth, and self-assembly of the inorganic particles.<sup>[8]</sup> All of the biomineralization synthesis routes have in common that they take place in water at ambient temperature and ambient pressure.

Cadmium chalcogenide nanoclusters (CdNCs) are one of the most fascinating types of fluorescent nanoclusters exhibiting molecule-like electronic behavior due to their ultrasmall size with several to tens of atoms in the core,<sup>[9]</sup> thereby possessing several potential applications in optics,<sup>[10]</sup> labeling,<sup>[11]</sup> and bioimaging.<sup>[12]</sup> Most of the studies so far relied on the synthesis of fluorescent CdNCs by using a common protein, i.e., bovine serum albumin (BSA)<sup>[13]</sup> which has 35 cysteines (Cys) out of a total of 583 amino acid residues. Moreover, BSA molecules are gaining attention not only due to the high numbers of metal-binding sites but also due to the exhibition of conformational changes, which lead to the accumulation of metal precursors into protein cages under alkaline conditions.<sup>[14]</sup> Unlike proteins with a large number of amino acids and Cys residues, small proteins without any Cys have not yet been used for the synthesis of fluorescent CdNCs.

Ubiquitin (Ub) is a small, cysteine-free protein with 76 amino acid residues (MW 8.565 kDa) that fold into a compact, globular, tightly hydrogen-bonded structure.<sup>[15]</sup> Although it has been used in some studies related to the interaction between proteins and nanoparticles,<sup>[16]</sup> its efficiency on the synthesis of CdNCs has never been investigated.

In this article, we studied whether Ub can be used for the synthesis of fluorescent CdNCs in water by utilizing the electrostatic interactions of Cd(II) via His68, Glu18, Glu16, Met1, Asp32, and Asp21 of Ub which can lead to the formation of trimers and oligomeric species due to metal bridges between dehydrons

Ö. Akyüz


Konstanz Research School Chemical Biology (KoRS-CB)  
University of Konstanz  
Konstanz 78457, Germany

Ö. Akyüz, Prof. H. Cölfen

Physical Chemistry  
Department of Chemistry  
University of Konstanz  
Konstanz 78457, Germany  
E-mail: helmut.coelfen@uni-konstanz.de

Prof. M. Scheffner

Department of Biology  
University of Konstanz  
Konstanz 78457, Germany

 The ORCID identification number(s) for the author(s) of this article can be found under <https://doi.org/10.1002/sstr.202000127>.

© 2020 The Authors. Small Structures published by Wiley-VCH GmbH. This is an open access article under the terms of the Creative Commons Attribution License, which permits use, distribution and reproduction in any medium, provided the original work is properly cited.

DOI: 10.1002/sstr.202000127

and protein domains.<sup>[17]</sup> We show that the synthesis of fluorescent cadmium selenide and cadmium sulfide nanoclusters (CdSeNCs and CdSNCs, respectively) is indeed possible by utilizing the small cysteine-free protein Ub. Analysis of the optical properties of CdSeNC@Ub and CdSNC@Ub was conducted with UV-Vis and fluorescence spectroscopy. The protein-metal interactions and size distributions were characterized by analytical ultracentrifugation (AUC) and high-resolution transmission electron microscopy (HR-TEM). Moreover, protein secondary structural changes and metal coordination efficiency of Ub were investigated with infrared spectroscopy (IR) and thermogravimetric analysis (TGA).

## 2. Results and Discussion

### 2.1. Characterization of CdSeNC@Ub and CdSNC@Ub

As shown in **Figure 1a**, CdSeNC@Ub shows broad range of absorption below 500 nm (represented by the black curve) and fluorescence emission (represented by the red curve) centered

at 600 nm. Moreover, CdSeNC@Ub can be efficiently excited by a diverse range of wavelengths below 360 nm without any significant changes to the emission maximum, indicating the stability of CdSeNC@Ub and real fluorescence from clusters rather than mere light scattering, which would show a  $1/\lambda^4$  dependence ( $\lambda$  = wavelength). The emission spectra for CdNCs@Ub are very typical for surface-related states that are strongly localized, typically in a single bond or ion. HR-TEM images (Figure 1c) indicate the formation of crystalline structures of CdSeNC@Ub in the average particle size of  $2.05 \pm 0.37$  nm. The second kind of cadmium chalcogenide synthesized in Ub is CdSNC@Ub, which exhibits a fluorescence emission band centered at 620 nm (represented by the red curve), which does not vary at the maxima when it is excited with different wavelengths (Figure 1b). HR-TEM investigation showed that the average particle size of the partly crystalline CdSNC@Ub is  $2.30 \pm 0.42$  nm (Figure 1d).

To further investigate the interactions between Ub and Cd(II), sedimentation velocity experiments of Ub and Cd(II) incubated Ub were performed by multiwavelength AUC (MW-AUC),<sup>[18]</sup>

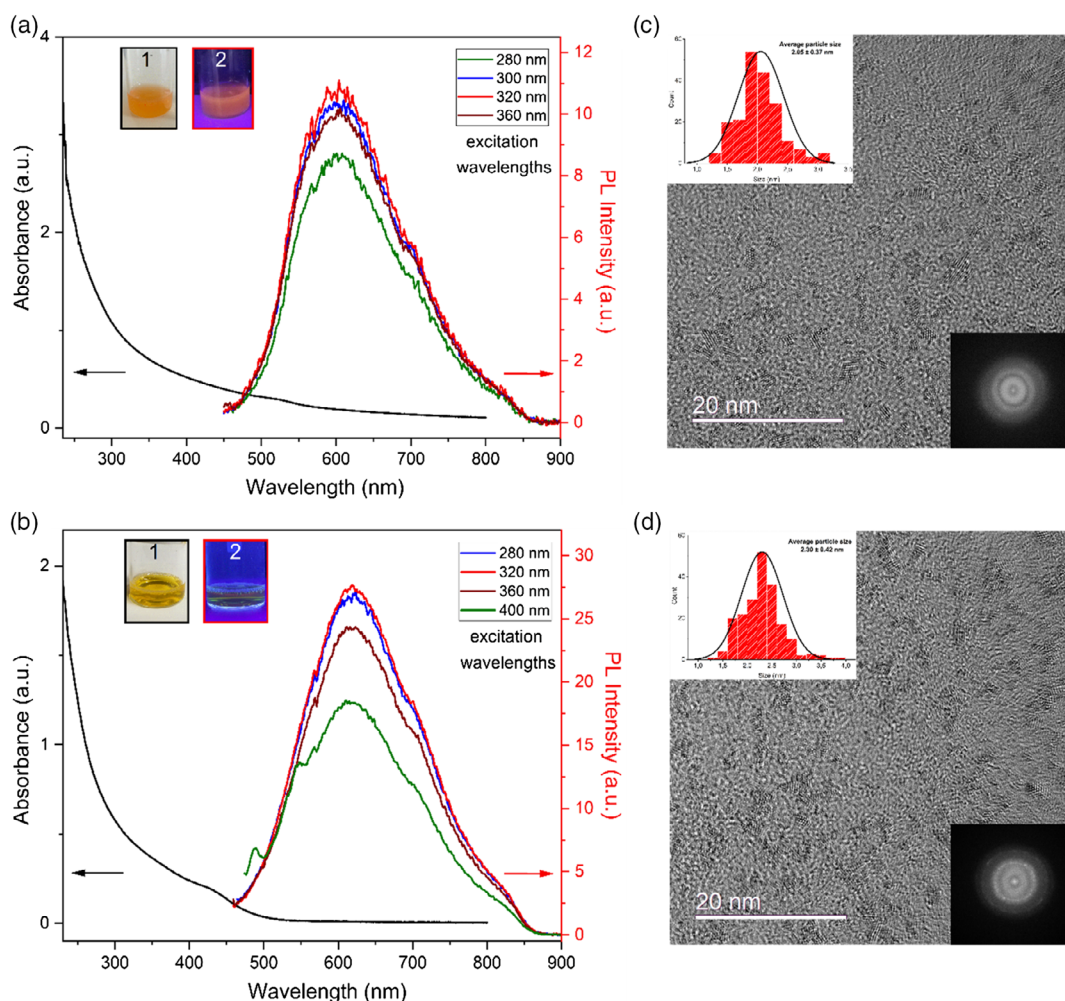


**Figure 1.** Absorption and emission spectra of a) CdSeNC, b) CdSNC in Ub, the insets include photographs of the clusters in visible light (1) and 365 nm light (2), HR-TEM images of c) CdSeNC@Ub and d) CdSNC@Ub, insets represent corresponding particle size histograms and selected area electron diffraction (SAED) patterns.

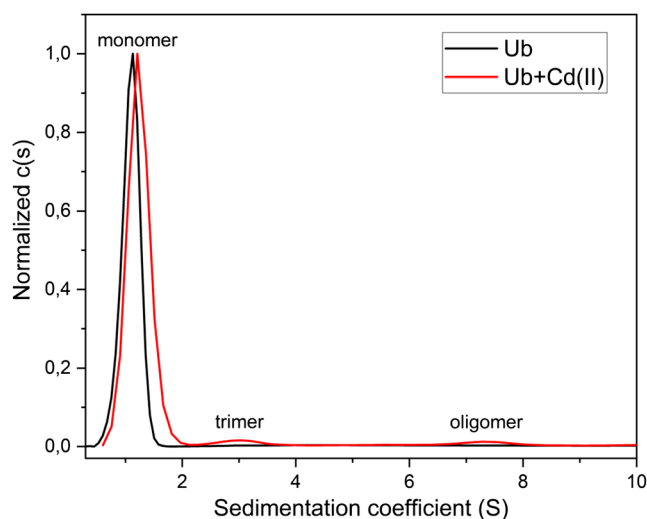


**Figure 2.** Diffusion broadening corrected sedimentation coefficient profile  $c(S)$  of Ub at pH 7 (black curve) and after incubation with Cd(II) (red curve).

which is one of the most robust techniques used to understand the structural properties of proteins<sup>[19]</sup> and any interactions with metals in solution.<sup>[20]</sup> As shown in **Figure 2**, the diffusion-corrected sedimentation coefficient distribution ( $c(S)$ ), represented by black curve) of Ub has a sharp peak with a sedimentation coefficient of 1.21 S, which reveals that there is no protein aggregation or oligomers at pH 7. In contrast, Ub which is incubated with Cd(II) at a 7:1 molar ratio at pH 7 exhibits two additional peaks at 3.06 and 7.34 S. After conversion of the sedimentation coefficient into the molecular mass distribution (see Figure S1, Supporting Information) using a partial specific volume of  $0.7257 \text{ cm}^3 \text{ g}^{-1}$  which was calculated according to the formula given in the Experimental Section, the results deduce that these two peaks are attributed to the formation of a trimer with 28.4 kDa and a higher oligomer, likely a 12-mer, with 105.9 kDa. In addition, the slight shift of the monomer peak to higher sedimentation coefficients with an otherwise unchanged peak indicates that the coordination of Cd(II) to Ub increases the density as well as the molar mass of the monomer, which results in the observed higher sedimentation coefficient.

The AUC results of Ub at different pHs, see **Table 1**, revealed another hydrodynamic parameter, the frictional ratio ( $f/f_0$ ),

**Table 1.** AUC parameters of Ub at three different pHs. ( $s_{20,w}$  is the sedimentation coefficient in water at  $20^\circ\text{C}$ ,  $\bar{v}$  is the partial specific volume of the protein,  $M_w$  is the molecular weight of the protein, and  $f/f_0$  is the frictional ratio.)

Parameters	Ub		
	pH 4	pH 7	pH 12
$s_{20,w}$ [s, $\times 10^{-13}$ ]	1.18	1.21	1.22
$\bar{v}$ [ $\text{cm}^3 \text{ g}^{-1}$ ]	0.735	0.735	0.735
$M_w$ [kDa]	8.27	8.38	8.68
$f/f_0$	1.28	1.33	1.33

which gives information about the degree of friction deviation from a minimum possible value of 1.0 for a hard sphere due to asymmetry, hydration, and expansion of the molecule. The frictional ratios of Ub lie in the range of 1.28–1.33, suggesting that it conserves the globular structure at acidic and alkaline conditions.

Interestingly, even though Ub does not undergo any conformational changes at basic conditions, the synthesis of CdSeNC@Ub at mild alkaline conditions (pH 8) resulted in a 50 nm blueshift in the fluorescent emission (**Figure 3a**) and in case of CdSNC@Ub (**Figure 3b**), no fluorescent particle formed at pH 8. This result demonstrates that the addition of NaOH is pivotal not only due to its effect on the conformation of the protein used, as observed, for example, for BSA<sup>[21]</sup>, but also to the activation of some acidic residues, which have the capacity to reduce metal precursors into NCs. For BSA, NaOH addition leads to conformational changes encapsulating the NCs under simultaneous activation of acidic residues, whereas in the here reported Ub case, the protein conformation remains unchanged so that the observed pH-induced change of the fluorescence emission wavelength (**Figure 3a**) is a result of the activation of the acidic amino acids, which then strongly interact with Cd(II).

To obtain more detailed information about the number of proteins incorporated with NCs, CdSeNC@Ub and CdSNC@Ub were measured in MW–AUC. Eventhough Ub has no changes in its conformation at alkaline conditions, incorporation with NCs would result in a different partial specific volume and likely also different frictional ratio than 1.33. This can also be explained by the predicted degree of hydration<sup>[22]</sup> for CdSeNC@Ub and CdSNC@Ub which are 2.40 and 3.35 g water per g solute, respectively. These values about a factor of 8–11 higher than the commonly accepted value of  $0.3 \text{ g g}^{-1}$  hydration for a monomolecular hydration layer around the protein and indicate a significant hydration of the NCs. As described in the Experimental Section, AUC data analysis, the partial specific volume of the whole structure, was evaluated by using the sedimentation coefficients in different solvents (e.g.,  $\text{H}_2\text{O}$  and  $\text{D}_2\text{O}$ ),<sup>[23]</sup> and the number of Ub for each species was calculated by using the methodology reported.<sup>[24]</sup> The values of the partial specific volume and total molecular mass of the NCs with protein shell (**Table 2** and **3**) provide details about the amount of monomeric and oligomeric species in the CdNCs solutions. The results reveal that CdSeNCs are formed with 16.80% of monomeric species of Ub, 28.3% NCs interact with the Ub tetramer, and almost the half amount of the NCs present with oligomeric species of Ub. Therefore, we conclude that CdSeNCs are directing the formation of mostly oligomeric species of Ub. Similarly, in case of CdSNC, almost 75.5% of the NCs are associated with oligomeric species of Ub.

To further explore the interaction of the Ub protein with clusters and potential secondary structural changes, the Fourier transform infrared–attenuated total reflection (FTIR–ATR) spectra were obtained. The amide A band near  $3250 \text{ cm}^{-1}$  arises mainly from the N–H stretching vibration in resonance with amide II, whereas amide I absorptions near  $1650 \text{ cm}^{-1}$  result primarily from the C=O stretching vibration of the amide group, and amide II absorptions near  $1650 \text{ cm}^{-1}$  are due to N–H bending and C–N stretching vibrations.<sup>[25]</sup> As shown in **Figure 4a**, the ratio between the amide I and amide II signals of Ub at pH 7,

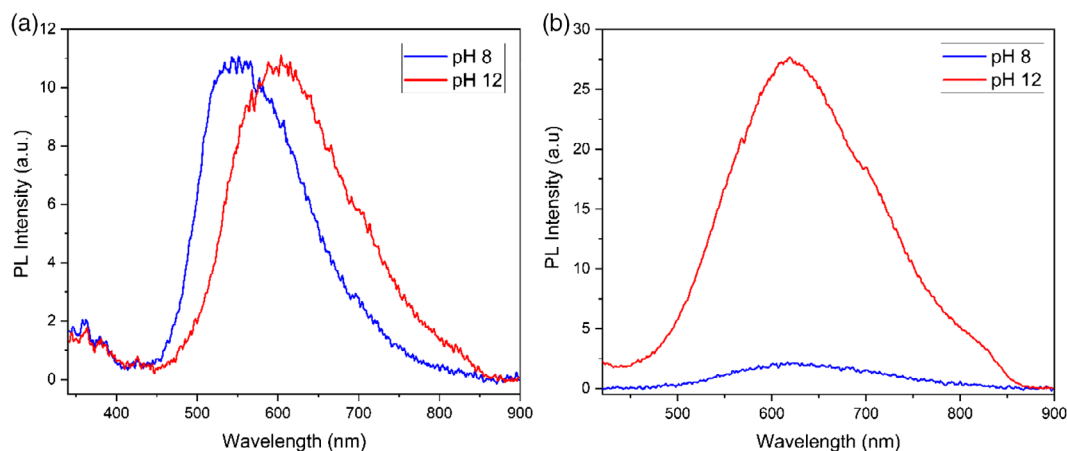


**Figure 3.** Fluorescent emission spectra of a) CdSeNC in ubiquitin (CdSeNC@Ub) and b) CdSNC in ubiquitin (CdSNC@Ub) excited with 320 nm light, synthesized at pH 8 (represented by the blue curve) and pH 12 (represented by the red curve).

**Table 2.** AUC results of each species (S) calculated in CdSeNC@Ub. ( $s_{20,w}$  is the sedimentation coefficient in water at 20 °C,  $\bar{v}$  is the partial specific volume of the cluster including protein,  $M_t$  is mass of the nanocluster with protein shell,  $N_{max}$  is the maximum number of proteins per NC, and  $P_s$  is the amount of each kind of species in solution.).

Parameters	CdSeNC@Ub		
	S1 (monomer)	S2 (tetramer)	S3 (oligomer)
$s_{20,w}$ [s, $\times 10^{-13}$ ]	$3.41 \pm 1.23$	$5.18 \pm 1.30$	$7.98 \pm 1.41$
$\bar{v}$ [ $\text{cm}^3 \text{g}^{-1}$ ]	$0.46 \pm 0.03$	$0.62 \pm 0.05$	$0.81 \pm 0.04$
$M_t$ [kDa]	$17.8 \pm 0.05$	$51.6 \pm 0.02$	$192.2 \pm 0.05$
$N_{max}$	$1.1 \pm 0.2$	$4.8 \pm 0.1$	$25.3 \pm 0.4$
$P_s$ [%]	16.80	28.30	54.90

**Table 3.** AUC results of each species (S) calculated in CdSNC@Ub. ( $s_{20,w}$  is the sedimentation coefficient in water at 20 °C,  $\bar{v}$  is the partial specific volume of the cluster including protein,  $M_t$  is mass of the nanocluster with protein shell,  $N_{max}$  is the maximum number of proteins per NC, and  $P_s$  is the amount of each kind of species in solution.).

Parameters	CdSNC@Ub		
	S1 (monomer)	S2 (oligomer)	S3 (oligomer)
$s_{20,w}$ [s, $\times 10^{-13}$ ]	$4.39 \pm 0.07$	$6.85 \pm 0.09$	$10.23 \pm 0.23$
$\bar{v}$ [ $\text{cm}^3 \text{g}^{-1}$ ]	$0.44 \pm 0.02$	$0.86 \pm 0.01$	$0.88 \pm 0.01$
$M_t$ [kDa]	$27.85 \pm 0.21$	$205.0 \pm 1.41$	$307.0 \pm 1.21$
$N_{max}$	$1.4 \pm 0.0$	$29.5 \pm 0.3$	$45.5 \pm 0.0$
$P_s$ [%]	24.50	19.50	56.00

pH 4, and pH 12 differs. This change in the amide I peak intensity indicates changes in the secondary structure of the protein. In addition, the decrease in the amide I peak intensity of CdSeNC@Ub and CdSNC@Ub can be attributed to not only the interactions of Ub with Cd(II) but also possible secondary structural changes taking place in Ub because of the reaction conditions and CdNCs incorporation. Therefore, for a deeper

understanding of each secondary structural component, amide I peak deconvolution was applied and each band was characterized according to protein-related studies reported before.<sup>[26]</sup> The results show that the helical content in Ub decreased from 27% to 15% and 18% at pH 4 and pH 12, respectively, and converted into sheets, turns, and coils (Figure 4b). CdSeNC@Ub and CdSNC@Ub have almost the same percentage of helical content as the NaOH-treated Ub. Although NaOH addition would convert some helical content into 10% more sheets, CdSeNC@Ub and CdSNC@Ub have less sheets in percentage of 55% and 50%, respectively. This might be explained by the interactions of CdNCs mostly with the beta sheets of Ub resulting in the formation of more turns and coils.

The TGA curves (Figure 5) for CdSeNC@Ub and CdSNC@Ub were determined from 30 to 1000 °C consisting of five stages. The first stage in both of the samples between 30 and 125 °C is due to the escape of water molecules. The second stage of weight loss in CdSeNC@Ub from 160 to 245 °C might be attributed to the decomposition of protein residues.<sup>[27]</sup> The derivative thermogravimetry of the next weight loss between 262 and 395 °C indicates that there are multiple stages rather than just one. The coordination of Ub to CdSeNC tends to enhance the thermal stability of Ub, suggesting that CdNCs interacting amino acid residues decompose at different temperatures during the third stage. The analysis of the weight loss percentage in stage 2 and 3 may provide the weight ratio between CdSe uncoordinated and coordinated Ub which is 3:10. Furthermore, the fourth stage from 396 to 520 °C with a weight loss of 7.5% could be attributed to the decomposition of CdSeNC. The last stage taking place between 585 and 916 °C can be assigned to the escape of the remaining oxidized selenium as gas. In case of CdSNC@Ub, the second stage (135–242 °C) with 6.5% weight loss may be due to the decomposition of uncoordinated Ub and the next multisteps between 247 and 325 °C with weight loss of 6.15% might be assigned to the decomposition of CdS coordinated Ub residues. In this article, the weight ratio between CdS uncoordinated and coordinated Ub is almost 1:1. The decomposition of the remaining material from 416 to 700 °C might be due to decomposition of CdSNC<sup>[28]</sup> and the

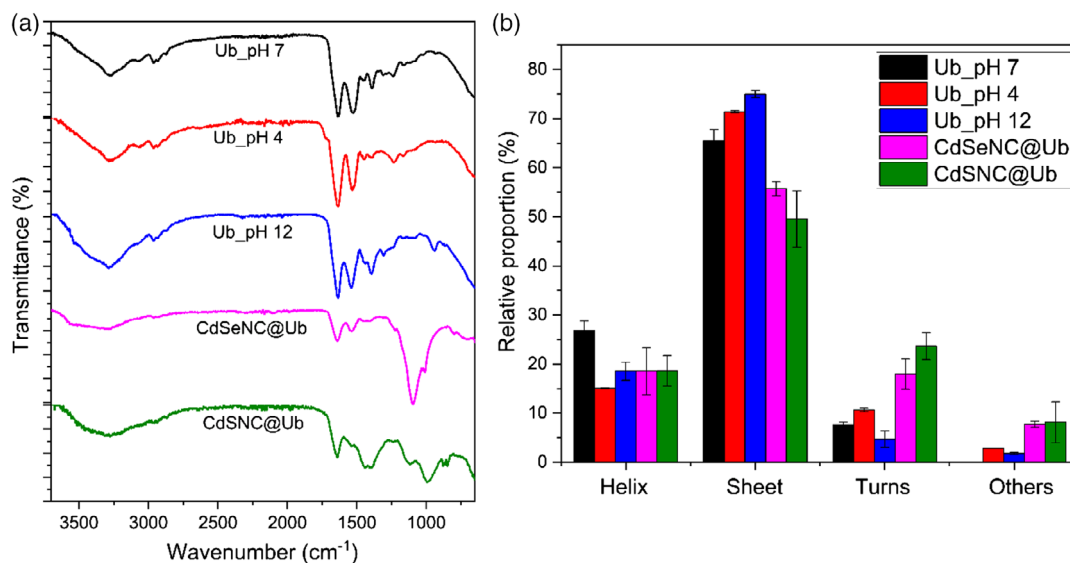


**Figure 4.** a) FTIR-ATR spectra, in amide A, amide I, and amide II regions and b) histogram illustrating the relative proportions of helix, sheet, turns, and others calculated in Ub at pH 7, pH 4, and pH 12, CdSeNC@Ub and CdSNC@Ub.

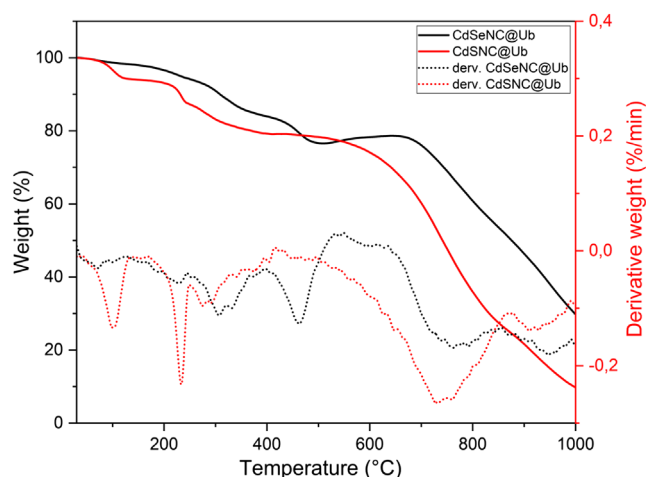


**Figure 5.** TGA and derivative TGA of CdSeNC@Ub and CdSNC@Ub.

weight loss between 700 and 900 °C can be attributed to the evaporation of oxidized sulfides.

### 3. Conclusion

In conclusion, we have reported the synthesis of fluorescent cadmium chalcogenides in Ub showing that the possibilities to obtain protein-stabilized nanoclusters go beyond BSA, which has been the standard for such investigations. The present results suggest that even a small cysteine-free protein, namely, Ub, has the potential to coordinate with CdNCs which results in fluorescence emission, secondary structural changes in Ub, Ub oligomerization, and enhancement of the thermal stability of Ub. We have also shown that the coordination of NCs changes

the structure of the protein as well as its oligomerization. The Ub embedded NCs are highly hydrated species according to AUC measurements.

### 4. Experimental Section

**Materials:** Milli-Q water (resistivity 18.2 mΩ cm) was used in all experiments. Ubiquitin from bovine erythrocytes (Ub), sodium hydroxide granules (NaOH), cadmium chloride (CdCl<sub>2</sub>), and sodium sulfide (Na<sub>2</sub>S) were purchased from Sigma-Aldrich. Selenide (Se) and sodium sulfite (Na<sub>2</sub>SO<sub>3</sub>) were obtained from Merck and Carl Roth, respectively.

**Synthesis of CdSeNC@Ub:** Ub solution was prepared in different concentrations (from 2.8 to 5.6 mg mL<sup>-1</sup>, 0.5 mL) and added to the CdCl<sub>2</sub> solution (from 0.04 to 0.02 mM, 0.5 mL) under N<sub>2</sub> protection. After 10 min at 37 °C, NaOH (0.5 M) was introduced and stirred for 30 min. After 5 h static incubation, Na<sub>2</sub>SeSO<sub>3</sub> solution (25 mM, 0.5 mL), which was freshly synthesized according to the reported procedure,<sup>[13b]</sup> was added and stirred overnight at 37 °C. The CdSeNC@Ub was dialyzed in a dialysis membrane (cutoff 1 kDa) against Milli-Q water at room temperature for the purification.

**Synthesis of CdSNC@Ub:** Ub (12 mg mL<sup>-1</sup>, 250 μL) was added to CdCl<sub>2</sub> solution (0.04 M, 0.75 mL) under N<sub>2</sub> protection and stirred for 15 min at room temperature. After 5 h static incubation at 37 °C, Na<sub>2</sub>S solution (0.04 M, 0.5 mL) was introduced and pH was adjusted to 12 by adding NaOH. The reaction was let to proceed at 60 °C for 5 h. Finally, the purification was performed by dialysis (cutoff 1 kDa) against Milli-Q water at room temperature.

**Characterization of Fluorescent Nanoclusters in Ubiquitin:** UV-vis and fluorescence spectra were recorded using a Varian Cary 50 UV-Vis Spectrophotometer and Cary Eclipse Fluorescence Spectrophotometer, respectively. A JEOL JEM-2200FS-HR-TEM was used to characterize the size of the fluorescent nanoclusters. The TEM images were analyzed by using DigitalMicrograph (Gatan).

**Analytical Ultracentrifugation:** Sedimentation velocity experiments were conducted on a Beckman UV-vis MW-AUC<sup>[18]</sup> with Ti double sector cells having 0.3 cm centerpieces (Nanolitics GmbH, Potsdam) and sapphire windows. Ub samples (6 mg mL<sup>-1</sup>) and CdNC@Ub were prepared in 25 mM NaCl solution at proper pHs and performed at 20 °C and 60 krpm, with 300 scans and three averages.

**Data Analysis:** Density of Ub was calculated according to the formula  $\rho = 10^{24} M / (V N_A)$ , where  $\rho$  is the protein density in  $\text{g}/\text{cm}^3$ ,  $M$  is the molecular weight in  $\text{g}/\text{mol}$ ,  $V$  is the molecular volume in  $\text{\AA}^3$ , and  $N_A$  is Avogadro's number ( $6.022 \times 10^{23} \text{ mol}^{-1}$ ). The density of the overall structure with the core and protein shell was calculated by using the sedimentation coefficients of the sample in water and water/heavy water mixture at  $20^\circ\text{C}$ .<sup>[29]</sup> The number of protein for each species in CdSeNC and CdSNC solutions was calculated by using the Equation (1)<sup>[24]</sup>

$$N_{\text{protein}} = \frac{M_{\text{NC@Ub}} \rho_{\text{core}}^{-1} - M_{\text{NC@Ub}} \rho_{\text{NC@Ub}}^{-1}}{M_{\text{protein}} (\rho_{\text{core}}^{-1} - \rho_{\text{protein}}^{-1})} \quad (1)$$

with  $N_{\text{protein}}$  is number of protein per NCs,  $M_{\text{NC@Ub}}$  is total mass of the cluster with protein shell,  $\rho_{\text{core}}$  is the density of the core which is  $5.82$  and  $4.82 \text{ g cm}^{-3}$  for CdSe and CdS, respectively,  $\rho_{\text{NC@Ub}}$  is the density of the overall structure,  $M_{\text{protein}}$  is the mass of Ub, and  $\rho_{\text{protein}}$  is the density of Ub.

Data were evaluated three times with SEDFIT.<sup>[30]</sup> In SEDFIT, the  $ls\text{-}g^*(s)$  and  $c(s, D)$  analyses were used.<sup>[31]</sup> For the  $c(s)$  analysis, data were fitted with stimulated annealing using a confidence level ( $F$ -ratios) of  $0.9$  and a resolution of  $200$  grid points.  $ff/f_0$  values for Ub at different pHs were calculated by using 2D spectrum analysis (2DSA).<sup>[32]</sup> Percentage of monomer, tetramer, and oligomer of CdSeNC@Ub and CdSNC@Ub in solution were calculated by integrating the  $c(s, D)$  peaks of each CdNCs species in the distribution, which were fitted by using overall specific volumes.

**Attenuated-Total-Reflection Fourier-Transform Infrared Spectroscopy:** Attenuated-total-reflection Fourier-transform infrared spectroscopy (ATR-FTIR) was used to investigate interactions of the protein with nanoclusters and the effect of different pHs and CdNCs formation on the secondary structure of Ub. The amide I peak deconvolution was applied with use of the Gaussian/Lorentzian profile to each of the spectra from  $1550$  to  $1720 \text{ cm}^{-1}$  three times in origin. After best curve-fitting processes, the amount of each secondary structural component of Ub and CdSeNC@Ub and CdSNC@Ub was calculated from the relative area of the bands.

**Thermogravimetric Analysis:** The TGA measurements were performed with a Netzsch STA 449F3 Jupiter. The samples were measured at a temperature range of  $30\text{--}1000^\circ\text{C}$  with a heating rate of  $10 \text{ K min}^{-1}$ . The gas flow during the measurement consisted of  $254 \text{ mL min}^{-1}$  oxygen and  $250 \text{ mL min}^{-1}$  nitrogen.

## Supporting Information

Supporting Information is available from the Wiley Online Library or from the author.

## Acknowledgements

The authors thank Prof. Dr. Andreas Marx, Konstanz for useful discussions. This work was supported by the Konstanz Research School of Chemical Biology (KoRS-CB). The authors gratefully acknowledge the Deutscher Akademischer Austauschdienst (DAAD), graduate school scholarship program-2018, for financial support.

## Conflict of Interest

The authors declare no conflict of interest.

## Keywords

cadmium chalcogenide, fluorescent nanoclusters, small proteins, ubiquitin

Received: October 31, 2020  
Revised: December 12, 2020  
Published online: December 30, 2020

- [1] a) P. Couleaud, S. Adan-Bermudez, A. Aires, S. H. Mejias, B. Sot, A. Somoza, A. L. Cortajarena, *Biomacromolecules* **2015**, *16*, 3836; b) C. Guo, J. Irudayaraj, *Anal. Chem.* **2011**, *83*, 2883.
- [2] a) Q. Chen, L. Feng, J. Liu, W. Zhu, Z. Dong, Y. Wu, Z. Liu, *Adv. Mater.* **2016**, *28*, 7129; b) Y. Tao, Z. Li, E. Ju, J. Ren, X. Qu, *Nanoscale* **2013**, *5*, 6154.
- [3] Y. Kong, J. Chen, H. Fang, G. Heath, Y. Wo, W. Wang, Y. Li, Y. Guo, S. D. Evans, S. Chen, D. Zhou, *Chem. Mater.* **2016**, *28*, 3041.
- [4] Y. Feng, H. Wang, J. Zhang, Y. Song, M. Meng, J. Mi, H. Yin, L. Liu, *Biomacromolecules* **2018**, *19*, 2432.
- [5] a) A.-W. Xu, Y. Ma, H. Cölfen, *J. Mater. Chem.* **2007**, *17*, 415; b) A. Arakaki, K. Shimizu, M. Oda, T. Sakamoto, T. Nishimura, T. Kato, *Org. Biomol. Chem.* **2015**, *13*, 974.
- [6] a) R. A. McMillan, J. Howard, N. J. Zaluzec, H. K. Kagawa, R. Mogul, Y.-F. Li, C. D. Paavola, J. D. Trent, *J. Am. Chem. Soc.* **2004**, *127*, 2800; b) A. R. D. Voet, J. R. H. Tame, *Curr. Opin. Biotechnol.* **2017**, *46*, 14.
- [7] S. F. Adil, M. E. Assal, A. M. Khan, A. Al-Warthan, M. R. Siddiqui, L. M. Liz-Marzan, *Dalton Trans.* **2015**, *44*, 9709.
- [8] F. C. Meldrum, H. Cölfen, *Chem. Rev.* **2008**, *108*, 4332.
- [9] Y. Tao, M. Li, J. Ren, X. Qu, *Chem. Soc. Rev.* **2015**, *44*, 8636.
- [10] S. V. Gaponenko, *Optical Properties of Semiconductor Nanocrystals*, Cambridge University Press, Cambridge **2009**.
- [11] a) I. L. Medintz, H. T. Uyeda, E. R. Goldman, H. Mattoussi, *Nat. Mat.* **2005**, *4*, 435; b) X. Gao, W. C. Chan, S. Nie, *J. Biomed. Opt.* **2002**, *7*, 532.
- [12] a) M. Bruchez Jr, M. Moronne, P. Gin, S. Weiss, A. P. Alivisatos, *Science* **1998**, *281*, 2013; b) Y. Cui, C. Zhang, L. Song, J. Yang, Z. Hu, X. Liu, *J. Nanosci. Nanotechnol.* **2018**, *18*, 2271.
- [13] a) D. Ghosh, S. Mondal, S. Ghosh, A. Saha, *J. Mater. Chem.* **2012**, *22*, 699; b) P. Huang, L. Bao, D. Yang, G. Gao, J. Lin, Z. Li, C. Zhang, D. Cui, *Chem. Asian J.* **2011**, *6*, 1156; c) J.-G. Liang, X.-P. Ai, Z.-K. He, H.-Y. Xie, D.-W. Pang, *Mater. Lett.* **2005**, *59*, 2778.
- [14] a) Y. Yu, J. Geng, E. Y. Ong, V. Chellappan, Y. N. Tan, *Adv. Healthcare Mater.* **2016**, *5*, 2528; b) M. Ahmed, A. Guleria, M. C. Rath, A. K. Singh, S. Adhikari, S. K. Sarkar, *J. Nanosci. Nanotechnol.* **2014**, *14*, 5730.
- [15] X. Zhao, M. Scheffner, A. Marx, *Chem. Commun.* **2019**, *55*, 13093.
- [16] a) G. Brancolini, D. B. Kokh, L. Calzolai, R. C. Wade, S. Corni, *ACS Nano* **2012**, *6*, 9863; b) L. Calzolai, F. Franchini, D. Gilliland, F. Rossi, *Nano Lett.* **2010**, *10*, 3101.
- [17] G. Falini, S. Fermani, G. Tosi, F. Arnesanob, G. Natile, *Chem. Commun.* **2008**, *127*, 5960.
- [18] J. Pearson, J. Walter, W. Peukert, H. Cölfen, *Anal. Chem.* **2018**, *90*, 1280.
- [19] S. Unzai, *Biophys. Rev.* **2018**, *10*, 229.
- [20] J. B. Bailey, R. H. Subramanian, L. A. Churchfield, F. A. Tezcan, *Methods Enzymol.* **2016**, *580*, 223.
- [21] J. M. Dixon, S. Egusa, *J. Am. Chem. Soc.* **2018**, *140*, 2265.
- [22] C. R. Cantor, P. R. Schimmel, *Biophysical Chemistry, Part II: Techniques for the study of Biological Structure and Function*, W. H. Freeman and Company, New York **1980**.
- [23] a) H. G. Müller, F. Herrmann, *Prog. Colloid Polym. Sci.* **1995**, *99*, 114; b) S. J. Edelstein, H. K. Schachman, *J. Biol. Chem.* **1967**, *242*, 306; c) W. Machtle, *Makromol. Chem.* **1984**, *185*, 1025.
- [24] R. P. Carney, J. Y. Kim, H. Qian, R. Jin, H. Mehenni, F. Stellacci, O. M. Bakr, *Nat. Commun.* **2011**, *2*, 335.
- [25] a) M. Jackson, H. H. Mantsch, *Crit. Rev. Biochem. Mol. Biol.* **1995**, *30*, 95; b) A. Barth, *Biochim. Biophys. Acta* **2007**, *1767*, 1073.

- [26] a) F. Bonnier, S. Rubin, L. Debelle, L. Venteo, M. Pluot, B. Baehrel, M. Manfait, G. D. Sockalingum, *J. Biophotonics* **2008**, *1*, 204;  
b) X.-Y. Shi, J. X. D. Li, S. Wang, Z.-Q. Wu, H. Chen, *Chin. Sci. Bull.* **2012**, *57*, 1109.
- [27] L. Yang, R. Xing, Q. Shen, K. Jiang, F. Ye, Q. R. J. Wang, *J. Phys. Chem. B* **2006**, *110*, 10534.
- [28] S. Wageh, M. Maize, *J. Mater. Sci.: Mater. Electron.* **2014**, *25*, 4830.
- [29] S. J. Edelstein, H. K. Schachman, *Methods Enzymol.* **1973**, *27*, 82.
- [30] P. Schuck, *Biophys. J.* **2000**, *78*, 1606.
- [31] V. Mittal, A. Völkel, H. Cölfen, *Macromol. Biosci.* **2010**, *10*, 754.
- [32] E. Brookes, W. Cao, B. Demeler, *Eur. Biophys. J.* **2010**, *39*, 405.